applied sciences

MDPI

Article

Concrete Object Anomaly Detection Using a Nondestructive Automatic Oscillating Impact-Echo Device

Hsi-Chiang Chou

Department of Electrical Engineering, Tung Nan University, New Taipei 222, Taiwan; hcchou@mail.tnu.edu.tw; Tel.: +886-2-86625924

Received: 11 January 2019; Accepted: 26 February 2019; Published: 4 March 2019

Abstract: The goal of this study was to develop an impact-echo device that can conduct automatic oscillation tests, process signals rapidly, and apply it to concrete object anomaly analysis. The system presented in this study comprises three parts, namely the impact device, the oscillator circuit, and signal processing software. The design concept of the impact-echo device was inspired by a pendulum clock, and its implementation used a nondestructive wooden hammer instead of a conventional manual steel hammer. In this study, we used a pulse generator in the adjustable oscillator circuit to produce delayed changes. The delayed changes would activate the wooden hammer that struck the surface of the object. To process the signal, our lab used a built-in sound card in the computer to transfer the reflection soundwave from striking the wall to MATLAB software to analyze the energy of the frequency spectrum. This was conducted to evaluate whether the object contained anomalies and, if so, to determine the location of the anomalies to serve as a reference for real-life implementation.

Keywords: nondestructive; impact-echo device; concrete object; adjustable automatic oscillator; signal acquisition

1. Introduction

Concrete is commonly used in many types of construction and in a variety of configurations. Although materials scientists have been trying to improve the capabilities of concrete in recent years [1,2], the shrinkage of concrete, the differential settlement in a building's foundations, and the impacts of temperature stress and loading may cause cracks. In addition, the corrosion of reinforcing bars in concrete may lead to the development of longitudinal cracks along the bars. Cracks are the most common form of deterioration in concrete objects [3,4]. Moreover, Taiwan is located on the boundary of the Philippine Sea Plate and Eurasian Plate, where geotectonic movements are frequent, leading to severe or partial damage to the internal structure of buildings. The severity of such damage cannot be identified by sight, and, without repair, damaged structures may lead to large numbers of injuries and deaths. For example, several structures collapsed in recent years, including Houfeng Bridge in 2008, the Weiguan Building in 2016, and the Marshal Hotel in Hualian city (located on the east coast of Taiwan) in 2018, resulting in several casualties [5,6] and demonstrating the importance of structural safety inspections. Among the evaluation methods for structure damage, nondestructive structural safety evaluations have become increasingly popular. The advantage of a nondestructive testing method is that it does not cause damage to a building, and its implementation (online testing) does not interfere with the regular usage of the building. It is mobile, convenient, and can evaluate the internal deterioration condition of a structure in a short period of time. To date, the most common nondestructive test in civil engineering was developed using the theories of

electromagnetic waves and stress waves. For example, ground-penetrating radar uses electromagnetic testing technology [7–10], whereas the ultrasonic method and the impact-echo method involve stress wave testing technology [11–15]. The electromagnetic testing technology involves expensive equipment, namely transceiver signal devices, transceiver antennas, signal recorders, and analysis systems; consequently, it is typically used in geotechnical engineering or oil-mining engineering. When the testing objects are concrete structures, such as those in the present study, testing technologies based on stress wave theories are more suitable. In addition, the ultrasonic method involves preburied boreholes that cause damage to the structure of a building. Therefore, the impact-echo method has gradually become the leading technology in civil engineering for conducting concrete structure testing. In recent years, the implementation of the impact-echo method has become increasingly diverse. It is used to test internal anomalies in rod structures (e.g., beams and columns) or in the concrete lining structure in tunnels, to examine the quality of a concrete structure, and to test the minimum width and the depth of cracks in a concrete structure. However, the implementation of the impact-echo method typically involves a device generating an impact on the testing object, and subsequently using a digital receiver to acquire the echo wave signals and signal acquisition devices to transmit the signals to the computer for analysis [16–19]. For disaster prevention, however, fixed-point automatic detection and rapid signal processing are critical.

To improve the latencies, our lab developed a low-cost, labor-reducing, and real-time nondestructive testing system that can be applied as a mechanical impact method to determine whether a concrete object contains defects. The sound card used in our system transforms the data collected through the audio software interface, supplemented with MATLAB software [20], into the soundwave of the echo signals. Subsequently, the soundwaves are connected to the computer; the echo waves are acquired and reconstructed on a personal computer (PC). This system can directly transfer signals to a PC to process a substantial amount of data, which significantly reduced the time required for the acquisition and reconstruction of echo signals.

2. System Design

2.1. System Architecture

This study proposes an impact-echo detection system that automatically oscillates and rapidly processes data. In terms of the system's architecture, the hardware comprises an automatic oscillation impact device our lab designed for this study, and adjustable automatic oscillator circuits, while the software features an echo signal acquisition and structural anomaly analysis. The overall system framework is presented in Figure 1.

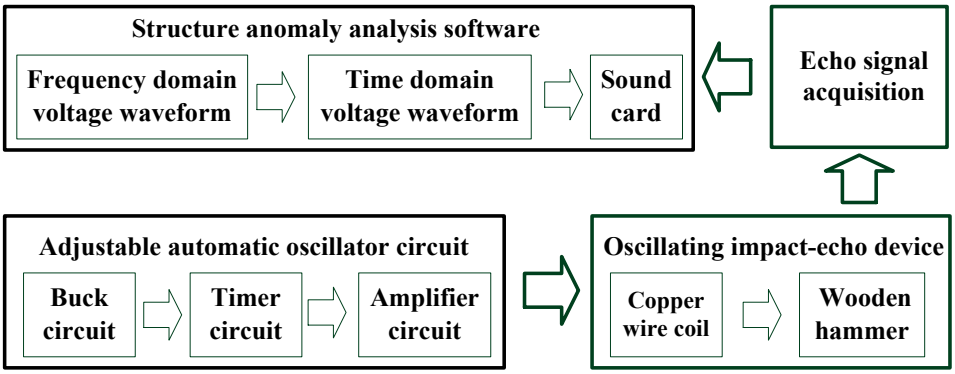

Figure 1. The overall system architecture.

2.2. Hardware Design

2.2.1. Adjustable Automatic Oscillator Circuit Design

The circuit of this study comprises a buck circuit, timer circuit, and amplifier circuit. The system produces continuous pulse outputs through energized coil and pig iron that generates electromagnetic effects and produces magnetic forces. Adjusting the frequency of the electric field produces a fixed force that activates oscillating impact-echo device to regularly generate impacts on a concrete object.

1. First-level buck circuit: For future applications, our lab designed the system based on simplicity, portability, and convenience. Thus, resistor–capacitor buck circuits were adopted to reduce volume and cost, and to replace cumbersome transformers. For rectification, a bridge rectifier that was composed of four 1N4007 diodes was adopted. Subsequently, nine 1K5W (1K Ohm can withstand 5 watts power) cement resistors that limit capacitance were connected to the charging current. Regarding filters, four 220V470uf (470 Farad can withstand 220 voltage) were used in the AC circuit; reactance caused by the capacitors resulted in the reduction of voltage to meet the voltage required for the electrical load. As for the voltage regulation, three 1K5W cement resistors were designed to be voltage dividers, and Zener diodes were used to maintain a specific voltage.
2. Second-level IC555 timer circuit: The output signal from the buck circuit of the previous level was 5 V, which could activate IC555 to produce modulation at periods ranging from microseconds to hours. Next, R1 and R2 (precision variable resistors) were used to adjust the frequency to generate a complete and continuous square wave signal.
3. Third level amplifier circuit: Because the output signal from the previous level had a low current value (5 V) and because the current amplification ratio of a single transistor was limited and could not drive the load of a large power system, two 2SC3457 transistors were used to construct an amplifier to improve high-frequency characteristics and prevent abnormal power loading from damaging the elements. Therefore, high power was acquired to drive enameled wire for charging or discharging. In addition, the on and off positions of two light-emitting diodes was used by our lab to indicate whether the amplifying circuit was connect. The overall amplifier circuit is illustrated in Figure 2.

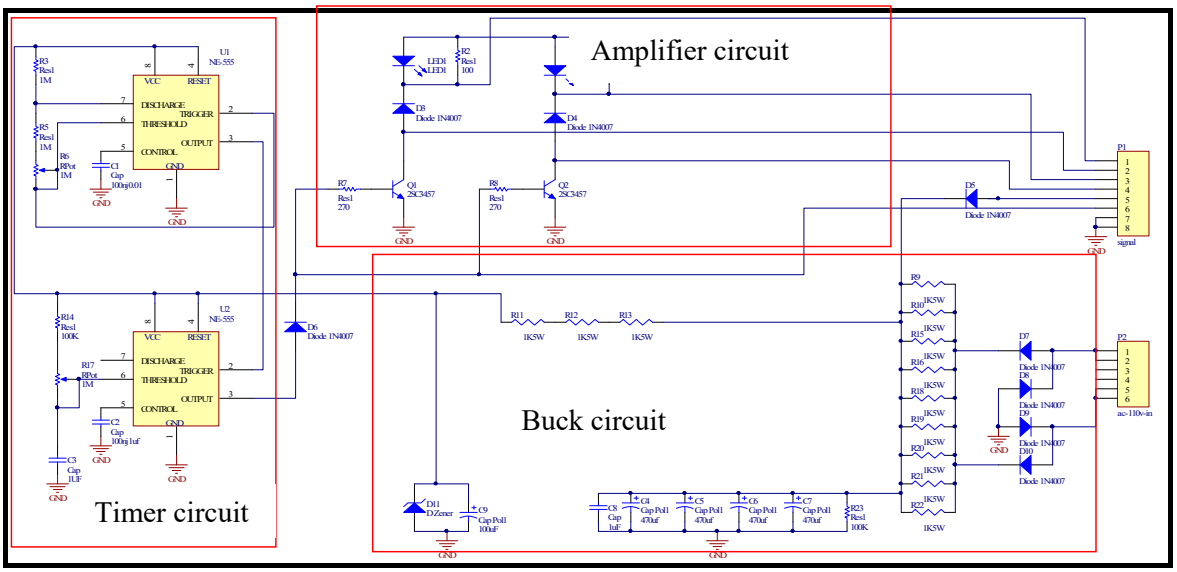

Figure 2. Overall circuit diagram.

Before the hardware (circuits) was connected to the software (the programs), it was required to undergo simulation and verification tests using Multisim (It is an electronic schematic capture

and simulation program. Production company location in Austin, Texas, USA) After the hardware system settings were finalized, the next step was to transmit echo signals to the computer program for anomaly analysis. The overall experimental setup is presented in Figure 3.

Figure 3. Experimental setup of the circuits.

2.2.2. Oscillating Impact-Echo Device

The oscillating impact-echo device contains an oscillating wooden hammer made of wood that strikes the wall. At the bottom of the wooden hammer, iron core made of pig iron was installed. In addition, an electromagnet device composed of two coils of enameled wire prepared for this study was erected.

1. Oscillating wooden hammer: First, the center point of the wooden hammer was identified, and then steel material was used to construct a computer numerical controlled lathe to fix the wooden hammer to the rotary machine and combine the steel material with the wooden material. The bearing was used as the fixed part in the impacting device to maintain the central position of its main body.
2. Copper wire coil: Enameled wire was prepared in this study to convert electromagnetic energy. Copper wire with insulation layers was rolled on cylindrical acrylic to form coils that were used in electromagnetic induction. Although more coils produce stronger magnetic force, saturation is eventually reached. To overcome the saturation of the magnetic force, an electric field tester and a current intensity meter were installed to test the electric field strength and the current intensity of the coils.
3. The bottom of the wooden hammer: Pig iron was used as the iron core, while magnetic force and coils was used to produce changes in magnetic flux that led to the induction of electromotive force. When the coils were not connected to electricity, no magnetic force occurred, so the electromotive force drove the electrons to generate induced current and subsequently achieve electromagnetic induction. The device has the same power to produce a 0.03 kg stable impacting force, as shown in Figure 4a.

After integrating the abovementioned rocking raft, winding coil, and the bottom of the raft, and a swinging tapper with a size of 35 cm × 15 cm × 32 cm, a weight of 1.7 kg was obtained. The physical system is shown in Figure 4b.

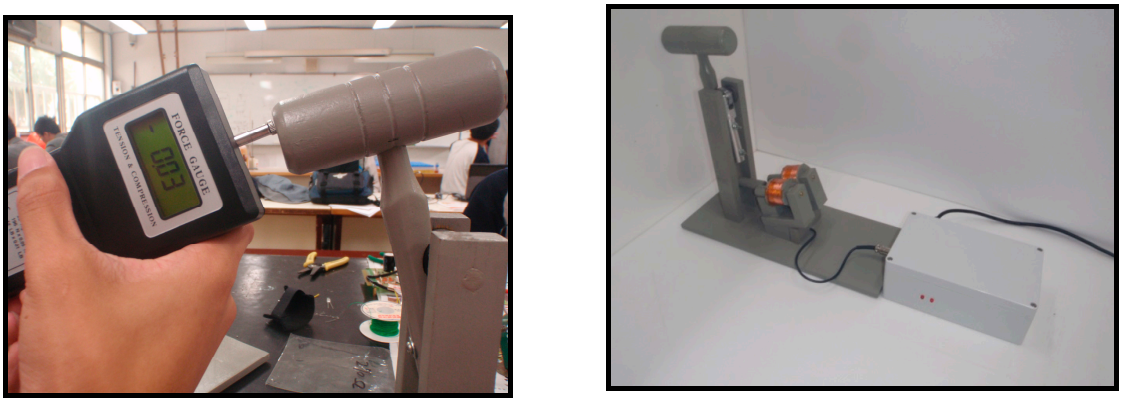

Figure 4. Experimental setup of the oscillating impact device: (**a**) physical system; (**b**) impacting force.

2.3. Software Design

2.3.1. Echo Signal Acquisition Processing

The sound card on the computer was used to transfer the echo soundwave, and GoldWave (It is a commercial digital audio editing software. Production company location in St. John's, Newfoundland, Canadian) audio editing software was used to produce an audio file [21]. For signal acquisition, a considerable number of data files were transferred directly to the PC to facilitate the construction of a measurements database in the future. The schematic of the hardware–software connection is illustrated in Figure 5.

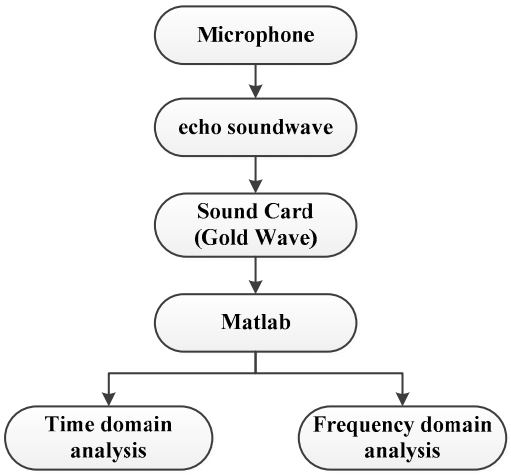

Figure 5. Schematic of hardware–software connection.

After the microphone acquired the echo soundwave (as analog signals) from the wooden hammer striking the test object, the GoldWave audio software acquired soundwave signals through the sound card (Figure 6).

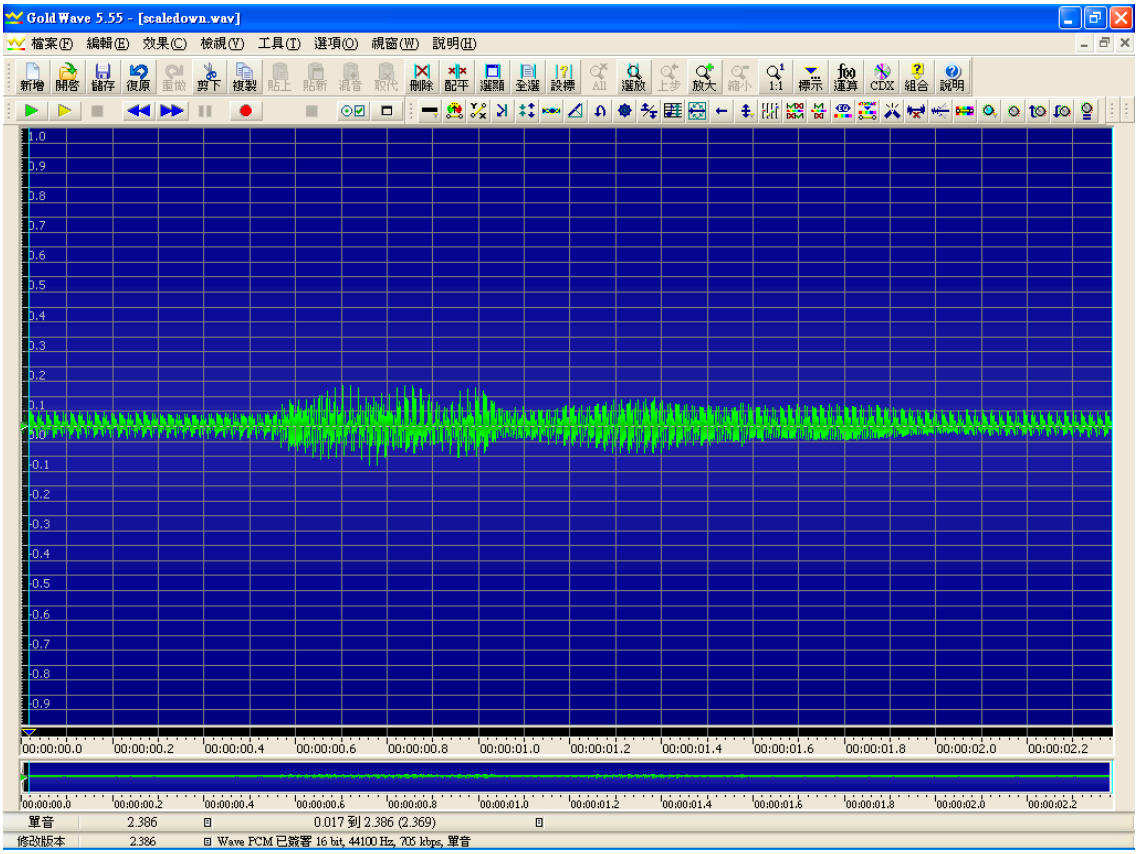

Figure 6. GoldWave acquired soundwave signals through the sound card.

2.3.2. Development of Object Anomaly Analysis Software

The anomaly analysis software was primarily developed using MATLAB. After the aforementioned echo signal was acquired and processed, the impact-echo signals stored in an audio file were translated to time domain and frequency domain programs to execute analyses using MATLAB software. The goal of the time domain analysis was to obtain the consecutive reflected waveforms from the impact device after the first reflected wave to evaluate the velocity of the soundwave. As for the frequency domain, substantial peaks were observed in the frequency graph. The established time frequency curve in the frequency graph was used to evaluate the structural anomaly in the object, which further confirms the accuracy of the analysis.

1. Time domain interface program design: Two string signals were tested. Their frequencies were 25 Hz and 200 Hz, and their amplitudes were 1.5 and 2.0, respectively. The discrete signal was sampled at 1 KHz, and 1000 samples were obtained. A portion of the codes for writing this signal and the acquired signals are presented in Figure 7.
2. Frequency domain interface program design: After conducting a Fast Fourier transform (FFT) of the time domain signals, we obtained frequency signals as shown in Figure 8. The frequency graphs revealed that at 25 Hz and 200 Hz, the amplitudes were 1.5 and 2.0, respectively.

When using FFT to obtain the spectrum of discrete signals, the maximum frequency that could be analyzed was half of the sampling frequency; when this frequency was exceeded, spectrum aliasing occurs, resulting in reading difficulties.

```
Fs = 1000;
T = 1/Fs;
L = 1000;
t = (0:L-1)*T;
y = 1.5*sin(2*pi*25*t)+2.0*sin(2*pi*200*t);
figure(1)
subplot(2, 1, 1);
plot(t, y)
title ('Signal (Full)')
xlabel ('time(milliseconds)')
subplot(2, 1, 2);
plot(t(1:200), y(1:200))
title ('Signal (0~0.05 Sec)')
xlabel ('time(milliseconds)')
```

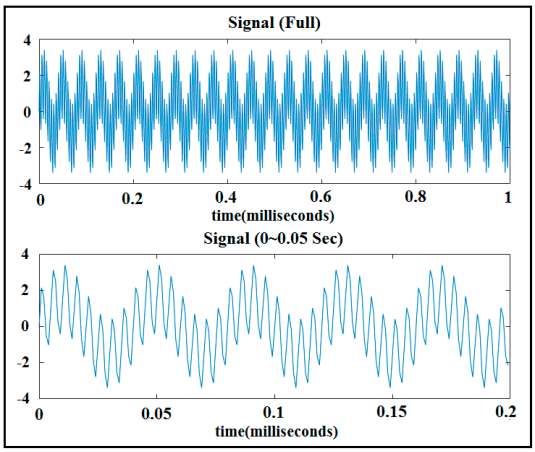

(**a**) (**b**)

Figure 7. Structural anomaly software development testing figures: (**a**) time domain program; (**b**) time domain signal graphs.

```
Y = fft(Y, L) / L;
F = Fs*linspace(0, 1, L);
Figure(2)
Subplot(2, 1, 1);
Plot(f, abs(Y(1:L)))
Title( 'Amplitude Spectrum of y(t)' )
xlabel( 'Frequency (Hz)' )
ylabel( '|Y(f)|' )
subplot(2, 1, 2);
plot(f(1:L/2), 2*abs(Y(1:L/2)))
title( 'Single-Sided Amplitude Spectrum of y(t)' )
xlabel( 'Frequency (Hz)' )
ylabel( '|Y(f)|' )
```

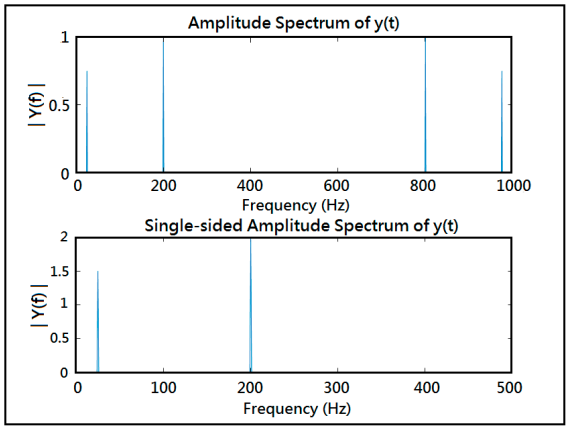

(**a**) (**b**)

Figure 8. FFT testing figures: (**a**) spectrum program; (**b**) spectrum graphs.

3. Experimental Setup Testing and Analysis Results

When a natural disaster happens, such as an earthquake, it often damages concrete structures, specifically creating cracks. It is critical to locate the cracks in a concrete structure in a timely manner to repair them and prevent the structure from incurring further damage. To address this issue, our lab developed an oscillation impact device and a signal acquisition and reconstruction system that can detect the location of a crack in a concrete object. In this section, the systematic integration of the module design is described in detail and the results of testing the experimental setup of the automatic oscillator circuit, oscillating impact device, echo signal acquisition device, and anomaly analysis programs are presented.

3.1. Experimental Setup and Procedure

3.1.1. Experimental Setup

The environmental setup included an oscillating impact device, automatic oscillator circuit, a notebook computer, a microphone, and concrete objects. The experimental setup of the overall system is shown in Figure 9. The environmental test of the experimental setup was divided into three

parts: (1) Using the automatic oscillator circuit to produce a continuous square wave and using the iron core of the oscillating impact device and the circuit to produce electromagnetic induction in order to perform automatic impacting. (2) Connecting the microphone to the sound card on the computer to transfer the original analog signals into digital signals. (3) Importing the audio files produced by the audio analysis software GoldWave into the self-developed MATLAB program to evaluate anomalies.

Figure 9. Experimental setup of the overall system.

3.1.2. Explanation of Experimental Procedure

The experimental procedure in this study followed the standard operating procedure of the impact-echo method and comprised the following steps:

(1) Wave velocity calculation: In this study, the wooden hammer was used as the impact echo device. when the impact echo device struck the concrete object that generated the first signal was considered the point of origin of the impact, and the first time when the echo wave reflected to the surface was considered the receiving point. The time lag between impact and reflection and the distance between the impact device and the echo signal acquisition device were used to calculate the velocity of the P-wave.

(2) Concrete object thickness test: When the impact echo device struck the surface of the concrete object, it produced echo waves that traveled downward until they reached the bottom of the concrete object. Once the echo waves reached the bottom of the object, they were reflected back to the surface of the concrete object. Then, the reflected wave created another reflected wave that continued to travel between the bottom and the surface of the concrete object, and thus multiple reflected waves were obtained to evaluate the thickness of the object.

(3) Concrete object internal defect detection: The same method as in point (2) above was used to detect the defects in the concrete object. When the echo waves were produced, the echo waves traveled downward until the waves reach the cracks in the concrete object. As the echo waves reach the cracks in the object, it reflected back to the surface of the concrete object. The reflected wave created another reflected wave that continued to travel between the locations of the cracks and surface of the concrete object. Therefore, multiple reflected waves were obtained to evaluate the internal defects of the object.

3.2. Concrete Object Crack Detection

Since the purpose of this study is to develop a system to detect the defects in a damaged concrete object in a timely manner and be able to use this system in real damaged structures such as buildings and bridges, our lab asked the concrete industry to produce regular and defective concrete objects. A total of one regular and two cracked objects were used for characteristic analysis (Table 1).

Table 1. Testing object characteristics.

Type		Thickness (cm)	Crack Depth (cm)
entry 1	Object 1	30	N/A
entry 2	Object 2	30	15
	Object 3	50	12

3.2.1. Regular Concrete Object (Object 1) Test

The characteristics tested were thickness and internal defections. Thickness testing was performed on both sides of the object, whereas internal defect testing was performed on only one side.

(1) Thickness test: The impact-echo device was used to strike one side of the studied object. The microphone collected the sounds, and the sound card processed the sound to form an audio file for MATLAB to conduct simulations. The obtained waveform graph is presented in Figure 10. Figure 10a presents the waveform of the incident impact point. Figure 10b depicts the waveform of the first reflected wave. It can be seen from the figure that t_1 is the impact time (243.3 μs), whereas t_2 is the reflected wave receiving time (257.7 μs). The time lapse is $t_2 - t_1$ = 14.4 μs. Because the distance between the impact device and receiver was 5 cm, the velocity of the P-wave was 3742 m/s. Figure 10c shows the overall reflected wave, which was simulated using MATLAB, and Figure 10d presents the wave frequency, which was obtained using FFT and indicates that the main frequency was 6.4 KHz. After calculation, dividing the wave velocity by twice the frequency revealed that the thickness of the object was approximately 28.1 cm, which was almost the same as the actual thickness of 30 cm. To verify the feasibility of this system, we also strike the other side of the studied object. Figure 11a presents the waveform of the incident impact point. Figure 11b shows the waveform of the first reflected wave. It can be seen from the figure that t_1 was the impact time (243.3 μs), whereas t_2 was the reflected wave receiving time (257.7 μs). The time lapse was obtained by subtracting t_1 from t_2 (14.4 μs). Because the distance between the impact device and receiver was 5 cm, the velocity of the P-wave was 3742 m/s. Figure 11c shows the MATLAB simulation of the reflected wave. Figure 11d presents the wave frequency graph obtained from FFT and main frequency was 6.1 KHz. The same calculation method revealed that the studied object thickness was approximately 29.5 cm, which was similar to the actual thickness of 30 cm. This object has performed a total of 10 measurements, which are measured five times on each side. The measured values on one side are 28.1 cm, 27.7 cm, 27.4 cm, 27.9 cm, and 28.9 cm. The other side of the measured values is 28.7 cm, 29.1 cm, 29.6 cm, 29.5 cm, and 29.8 cm. The average value of each side is close to 30 cm, which is the actual thickness of the studied object.

(2) Internal defect testing: This test was conducted on a regular concrete object without internal cracks (Object 1). The frequency domain waveforms in Figures 10d and 11d reveal the absence of continuous high-frequency reflected waves after the highest main frequency, so this Object was considered to contain no internal cracks.

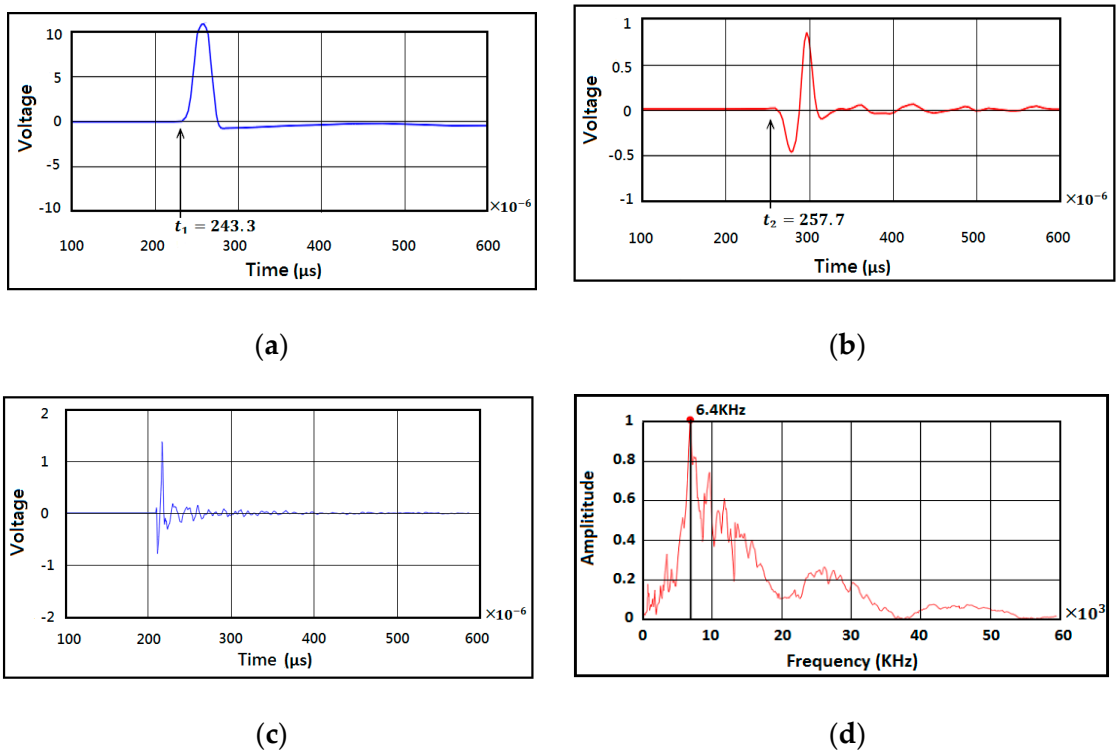

Figure 10. Regular concrete impact wave graph: (**a**) incident impact point wave graph; (**b**) first reflected wave waveform graph; (**c**) MATLAB simulation graph; (**d**) spectrogram.

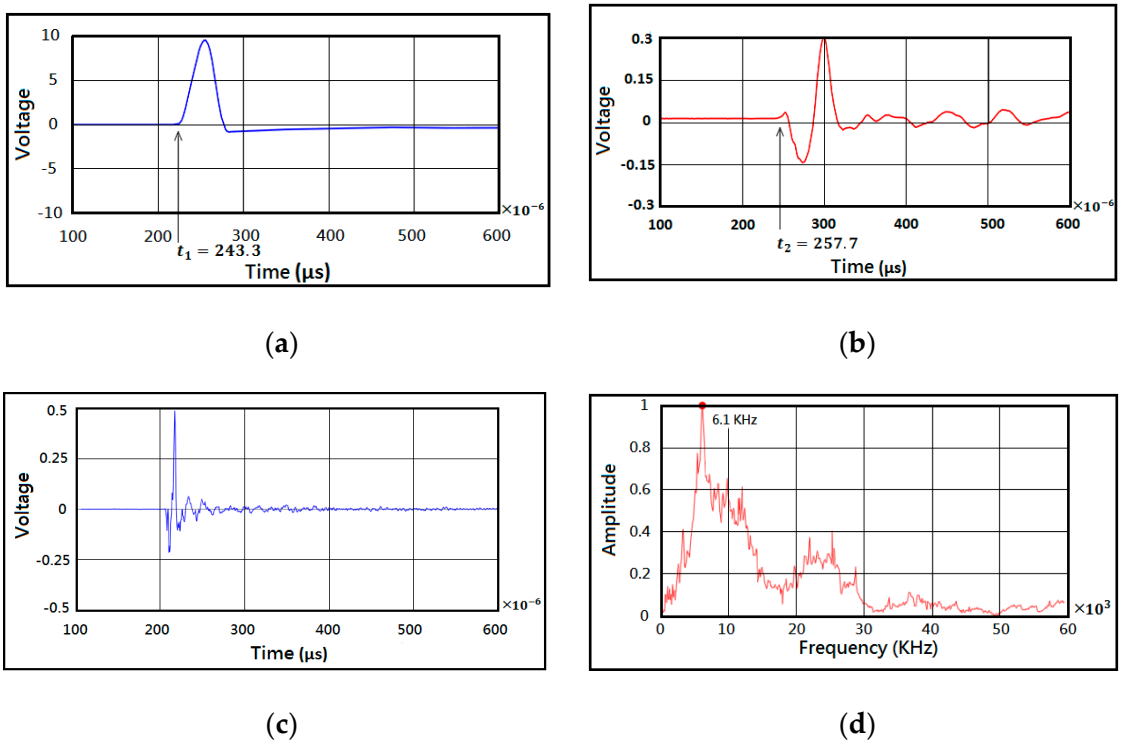

Figure 11. Regular concrete impact wave graph from striking the other side of the object: (**a**) incident impact point wave graph; (**b**) first reflected wave waveform graph; (**c**) MATLAB simulation graph; (**d**) spectrogram.

3.2.2. Testing a Concrete Object with Cracks (Object 2)

Object 2 was 30 cm in thickness with a crack 15-cm deep in the concrete. The impact-echo device struck one side of the studied object. The microphone was utilized to collect sounds, and the sound card processed the recording and produced the audio file to be imported into MATLAB for simulation, resulting in the waveform graph shown in Figure 12. Figure 12a presents the incident impact point wave graph. Figure 12b shows the waveform graph of the first reflected wave. The t_1 is the impact time (243.3 µs), whereas t_2 is the reflected wave receiving time (256.7 µs). The time lapse is expressed as $t_2 - t_1$ = 13.4 µs. Because the distance between the impact device and receiver was 5 cm, the velocity of the P-wave was 3748 m/s. Figure 12c presents the overall reflective wave from MATLAB simulation. Figure 12d reveals two pronounced frequencies, signal A at 6.1 KHz and signal B at 12.4 KHz obtained using FFT. A thickness of 29.5 cm and a crack depth of 14.5 cm were obtained in this study calculated by the wave velocity of 3748 m/s. A total of six crack depth measurements were performed in this object and the measured values were 14.3 cm, 14.5 cm, 13.9 cm, 14.6 cm, 15.3 cm, and 14.8 cm. The average value of the crack depth matched the actual crack depth of the studied object that was originally manufactured by the concrete industry.

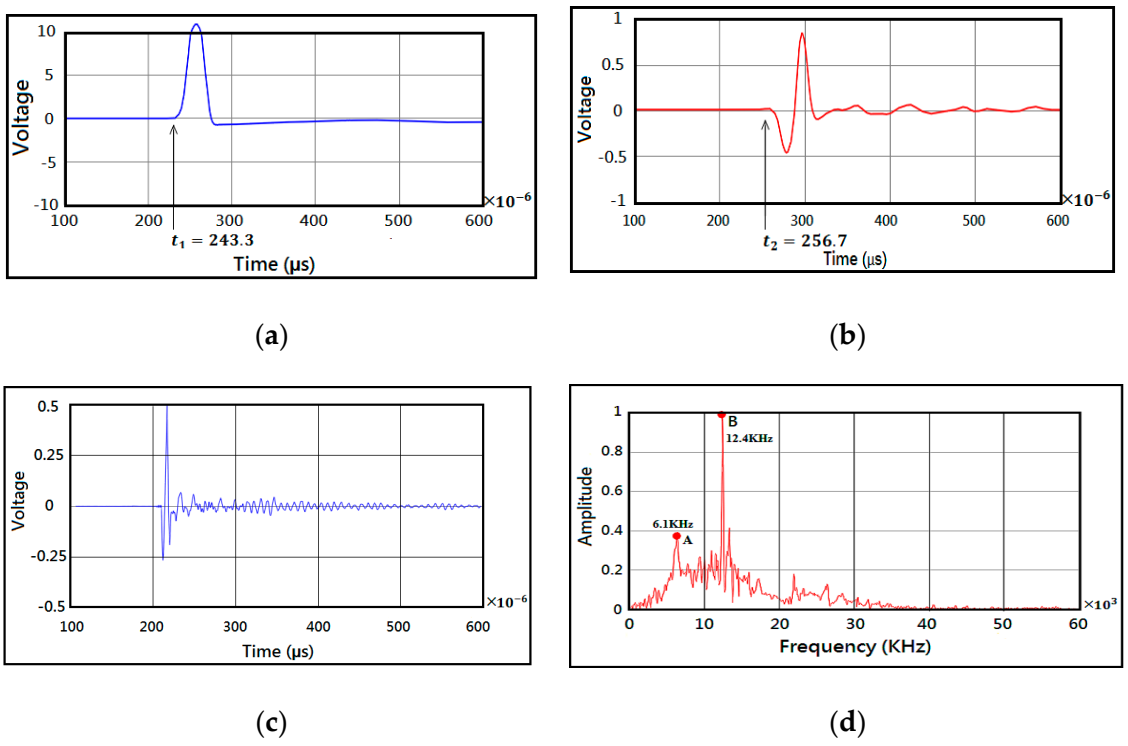

Figure 12. Impact wave graph of object 2 with a crack depth of 15 cm: (**a**) incident impact point wave graph; (**b**) first reflected wave waveform graph; (**c**) MATLAB simulation graph; (**d**) spectrogram.

3.2.3. Concrete Object with Cracks (Object 3) Testing

Object 3 was 50 cm in thickness with a crack 12 cm deep in the concrete. The impact-echo device struck one side of the studied object. The microphone was utilized to collect the sounds, and the sound card processed the recording and produced the audio file to be imported into MATLAB for simulation, resulting in the waveform figure shown in Figure 13. Figure 13a depicts the incident impact point wave graph. Figure 13b presents a waveform graph of the first reflected wave. The t_1 is the impact time (243.3 µs), whereas t_2 is the reflected wave receiving time (256.7 µs). The time lapse is expressed as $t_2 - t_1$ =13.4 µs. Because the distance between the impact device and receiver was 5 cm, the velocity of the P-wave was 3748 m/s. Figure 13c presents the overall reflective wave from the MATLAB simulation. Figure 13d reveals two conspicuous frequencies, signal A at 3.8 KHz and signal

B at 13.7 KHz obtained using FFT. A thickness of 49.3 cm and a crack depth of 13.6 cm were obtained in this study calculated by the wave velocity of 3748 m/s. In addition, at 7.3 KHz, the amplitude was the same as that of Signal B at 13.7 KHz, at a depth of approximately 23.9 cm, possibly resulting from an internal defect at the bottom of the concrete. A total of five crack depth measurements were performed in this studied object, and the measured values were 12.7 cm, 14.1 cm, 13.9 cm, 13.6 cm, and 13.3 cm. The average value of the crack depth matched the actual crack depth of the studied object that was originally manufactured by the concrete industry.

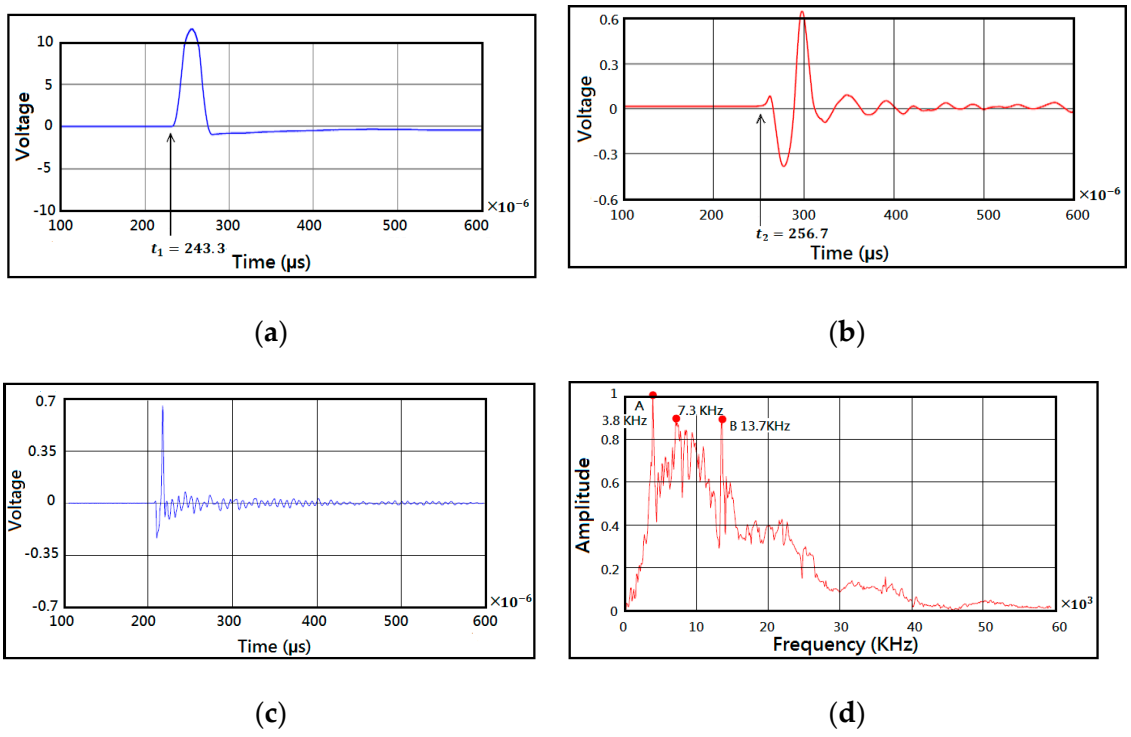

Figure 13. Impact wave graph of Object 3 with a crack depth of 12 cm: (**a**) incident impact point wave graph; (**b**) first reflected wave waveform graph; (**c**) MATLAB simulation graph; (**d**) spectrogram.

The testing results from the regular concrete object (Object 1) and cracked concrete objects (Object 2 and 3) were organized by their thickness, P-wave velocity, main frequency, measured crack depth, and error in Table 2.

Table 2. Data of testing objects.

Type		Object Thickness/Crack Depth (cm)	P-Wave Velocity (m/sec)	Main Frequency (KHz)	Measured Thickness/Crack Depth (cm)	Error of Thickness/Crack Depth
Regular	Object 1 (right)	30/NO	3742	6.4	28.1/NO	6.3%/0
	Object 1 (left)	30/NO	3742	6.1	29.5/NO	1.6%/0
Cracked	Object 2	30/15	3748	6.1 12.4	29.5/14.5	1.6%/3.3%
	Object 3	50/12	3748	3.8 13.7	49.3/13.6	1.4%/13%

4. Conclusions

The main purpose of this study was to develop an automatic oscillating impact-echo device that can rapidly process signals and reconstruct the measured signal waveform into a PC. The results of our study indicate that our self-developed system significantly reduces the time spent locating the cracks of a damaged building. Furthermore, the main contributions of this study are (1) a lightweight, low-cost, and ready-to-measure automatic oscillating impact-echo device to replace traditional complex and manual steel hammers and reduce the damage to buildings; (2) using the sound card in the personal computer to retrieve the echo signal, replacing the traditional expensive digital echo collector; (3) a complete automatic oscillating impact-echo device to connect with a personal computer, and analyze the tapping wave characteristics through the computer and transmit it to the remote network through the Internet; and (4) the automatic oscillating impact-echo device can do fixed-point testing, which is very helpful for the safety of the staff and saving manpower.

Funding: This research received no external funding.

Conflicts of Interest: The author declares no conflicts of interest.

References

1. Meng, W.; Khayat, K.H. Flexural Behaviors of Fiber-Reinforced Polymer Fabric Reinforced Ultra-High-Performance Concrete Panels. *Cem. Concr. Compos.* **2018**, *93*, 43–53. [CrossRef]
2. Meng, W.; Khayat, K.H. Effect of Graphite Nanoplatelets and Carbon Nanofibers on Rheological Properties, Hydration, Shrinkage, Mechanical Properties, and Microstructure of UHPC. *Cem. Concr. Res.* **2018**, *105*, 64–71. [CrossRef]
3. Bao, Y.; Valipour, M.; Meng, W.; Khayat, K.H.; Chen, G. Distributed Fiber Optic Sensor-Enhanced Detection and Prediction of Shrinkage-Induced Delamination of Ultra-High-Performance Concrete Bonded Over an Existing Concrete Substrate. *Smart Mater. Struct.* **2017**, *26*, 85–94. [CrossRef]
4. Bao, Y.; Meng, W.; Chen, Y.; Chen, G.; Khayat, K.H. Measuring Mortar Shrinkage and Cracking by Pulse Pre-Pump Brillouin Optical Time Domain Analysis with a Single Optical Fiber. *Mater. Lett.* **2015**, *145*, 344–346. [CrossRef]
5. Hong, J.H.; Chiew, Y.M.; Lu, J.Y.; Lai, J.S.; Lin, Y.B. Houfeng Bridge Failure in Taiwan. *J. Hydraul. Eng.* **2012**, *138*, 186–198. [CrossRef]
6. Hwang, S.J.; Chung, L.L.; Chiou, S.B.; Chen, H.T. Suggestions on Establishing a Law for Private Building Seismic Reinforcement. *J. Chin. Inst. Civ. Hydraul. Eng.* **2018**, *45*, 8–14. [CrossRef]
7. Harry, M.J. *Ground Penetrating Radar Theory & Application*, 1st ed.; Elsevier Science: Amsterdam, The Netherlands, 2009; pp. 1–40. ISBN 978-0-444-53348-7.
8. Basile, V.; Carrozzo, M.T.; Negri, S.; Nuzzo, L.; Villani, A.V. A ground-penetrating radar survey for archaeological investigations in an urban area. *J. Appl. Geophys.* **2000**, *44*, 15–32. [CrossRef]
9. Gary, R.O. Maximizing the information return from ground penetrating radar. *J. Appl. Geophys.* **2000**, *43*, 175–187. [CrossRef]
10. Redman, J.D. Assessment of Agricultural Drainage Pipe Conditions Using Ground Penetrating Radar. *J. Environ. Eng. Geophys.* **2010**, *15*, 119–134. [CrossRef]
11. Carino, N.J. Impact-echo Method. In Proceedings of the 2001 Structures Congress & Exposition, Washington, DC, USA, 21–23 May 2001.
12. Cheng, C.C.; Yu, C.P.; Chang, H.C. On the feasibility of deriving transfer function from Rayleigh wave in the impact-echo displacement waveform. *Key Eng. Mater.* **2004**, *270*, 1484–1492. [CrossRef]
13. Sansalone, M.; Carino, N.J. *A Microcontroller-Based Instrument for Measuring P-Wave Speed in Impact-Echo Testing of Concrete*; Institute of Electrical and Electronics Engineers: Hong Kong, China, 2006; pp. 14–17.
14. Yeh, P.L.; Liu, P.L. Application of the Wavelet Transform and the Enhanced Fourier Spectrum in The Impact Echo Test. *NDT E Int.* **2008**, *41*, 382–394. [CrossRef]
15. Itoh, S.; Hokamoto, K.; Fujita, M. A Method of Detecting Voids under Concrete Plates by Impact-Echo Test. *Mater. Sci. Forum* **2004**, *41*, 349–354. [CrossRef]

16. Katarzyna, K.; Izabela, H.R. Post-Fire Assessment of Mechanical Properties of Concrete with the Use of the Impact-Echo Method. *Constr. Build. Mater.* **2015**, *96*, 155–163. [CrossRef]
17. Gabriella, E.; Proverbio, E.; Venturi, V. Evaluation of Fire-Damaged Concrete Using Impact-Echo Method. *Mater. Struct.* **2009**, 1–11. [CrossRef]
18. Erik, B. Advance in Shotcrete Impact Testing. In *Shotcrete: Elements of System*; CRC Press: Boca Raton, FL, USA, 2010; Volume 41, pp. 111–117.
19. Grosse, C.U.; Reinhardt, H.W.; Beutel, R. Impact-Echo Measurement on Fresh and Hardening Concrete. *Concr. Sci. Eng.* **2004**, 95–104. [CrossRef]
20. Steven, C.C. *Applied Numerical Methods with MATLAB for Engineers and Scientists*, 2nd ed.; McGraw-Hill: New York, NY, USA, 2008; ISBN 978-007-125921-7.
21. Barry, P.; Marcia, P. *PC Toys: 14 Cool Projects for Home, Office, and Entertainment*; John Wiley & Sons Inc.: Hoboken, NJ, USA, 2003; ISBN 978-0764542299.